

High-Gain Persistent Nonlinear Conductivity in High-Voltage Gallium Nitride Photoconductive Switches

E. A. Hirsch, A. Mar, F. J. Zutavern, G. Pickrell, J. Delhotal, R. Gallegos, V. Bigman
Sandia National Laboratories
Albuquerque, New Mexico, USA

J. D. Teague, J. M. Lehr
Department of Electrical and Computer Engineering
University of New Mexico
Albuquerque, New Mexico, USA

Abstract— Wide-bandgap GaN optically-controlled switches have the potential for driving down the cost and size, and improving the efficiency and capabilities of high voltage pulsed-power applications. 600 μm gap devices were fabricated and laser tested from GaN wafers from Kyma and Ammono. With relatively low voltages applied the switch, linear photoconductive currents are measured through the pulse in response to exposure to the laser pulses. As increasing voltage is applied to the PCSS, above a threshold persistent conductivity is measured that lasts well beyond the duration of the laser pulse and discharges the charged transmission line in the system. This occurs at threshold fields of approximately 20 kV/cm. This persistent photoconductivity is a distinguishing characteristic of what is known as “lock-on” effect in photoconductive switches, most notably known in GaAs-based devices. This effect is the basis for highly-efficient photoconductive switching requiring relatively little laser energy. High-gain switching has been initiated in GaN devices with as little as 33 μJ laser energy thus far. Another distinguishing characteristic of lock-on switching effect known from characterization in GaAs is the formation of filamentary current channels. These filaments can be imaged due to the emission of recombination radiation from electrons and holes in the plasma within the filaments, and have been recorded in the GaN switches.

Keywords—photoconductive semiconductor switch; gallium nitride; photoconductive switching; wide-bandgap

I. INTRODUCTION

There is a vast need for fast high voltage switches to be used in power electronics and pulsed power applications. Wide bandgap (WBG) semiconductor materials have multiple advantages over typical semiconductors that have helped significantly advance high voltage switching over the last decade [1]. Table 1 shows the superior material properties of SiC and GaN to Si or GaAs for high voltage switching, namely their wide bandgap and breakdown field. GaN, specifically, has the largest bandgap, which results in less thermally generated carriers, a high breakdown field, which results in smaller device widths for similar breakdown voltages in Si or GaAs devices, and a mid-range thermal conductivity, which allows for elevated temperature operation of GaN PCSS. These parameters lead towards smaller systems with smaller devices and less thermal management requirements.

Wide bandgap semiconductor switches have been researched with various materials (SiC, GaN, etc.) and various transistors (diodes, MOSFETs, IGBTs, thyristors, HEMTs,

etc.). Typical state of the art WBG MOSFETs have a switching time in the hundreds of nanoseconds to tens of microseconds, but PCSS switches could switch in the single to tens of nanoseconds range, which allows for higher frequency switching in power electronics applications and decreases the physical size of components in the system [2-4]. State of the art switches in the market today can hold off approximately 15-20 kV and to reach the required high voltage hold off typical of power electronics for dc transmission, multiple switches need to be stacked in series, which comes with complex gate drive systems, whereas photoconductive semiconductor switches are optically controlled, which removes the requirement of floating gate driver systems [1].

II. DEVICE FABRICATION AND PCSS DEVICE PROPERTIES

A. Device Fabrication Overview

Semi-insulating GaN wafers were received from Kyma Technologies and Ammono. The Kyma Technologies wafer material is research grade semi-insulating GaN with HVPE growth. Figure 1(a) shows a number of surface defects visible by eye. The wafers are provided in 10 mm x 10 mm size with a thickness of approximately 475 μm . The resistivity of the Kyma wafers is quoted to be greater than $10^6 \Omega\text{-cm}$ and the dislocation density is quoted to be less than $5 \times 10^6 \text{ cm}^2$. The Ammono wafer material is a semi-insulating GaN with Ammonothermal growth. There are no large defects seen on the surface, as shown with Figure 1(b). The Ammono wafers were provided in 37.9 mm diameter wafers with a thickness of approximately 350 μm . The resistivity of the Ammono wafers is quoted to be greater than $10^9 \Omega\text{-cm}$ with a dislocation density less than $5 \times 10^4 \text{ cm}^2$.

TABLE I. MATERIAL PROPERTIES COMPARISON

Properties	Si	GaAs	4H SiC	GaN
Bandgap (eV)	1.11	1.43	3.26	3.42
Dielectric constant	11.8	12.8	9.7	9
Breakdown field (MV/cm)	0.25	0.35	3.5	3.5
Thermal conductivity (W/cm*K)	1.5	0.46	4.9	1.7

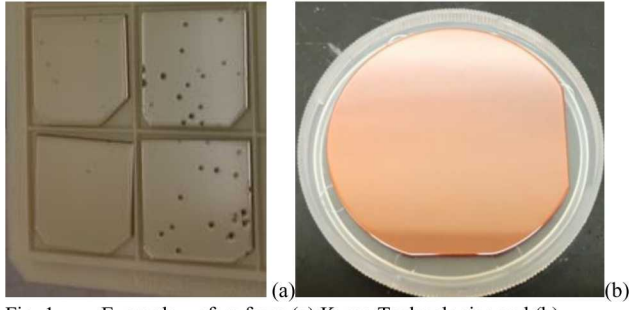


Fig. 1. Example wafers from (a) Kyma Technologies and (b) Ammono.

The first wafer mask design was based to test the material properties of the GaN from each manufacturer. The wafer was split into a wafer probe section and singulated die section with gap spacings of 25, 50, 100, 300, and 600 μm in the wafer probe section and 12 devices with 600 μm gap spacing in the singulated die section. Figure 2 shows a 600 μm gap singulated device with two gold ribbons bonded to each electrode. The singulated die was ribbon bonded to test boards for in-circuit testing and the wafer probe section was used to test multiple material parameters, such as the dark leakage current and surface flashover electric field of the material.

B. Dark Leakage Current

The devices were tested for their leakage current during voltage holdoff without laser light illuminating the device gap, also called “dark” leakage current. Devices made from both manufacturers were tested and compared. Figures 3 and 4 below show the leakage current for two each of Ammono and Kyma devices. The Ammono devices were tested with a 3 kV, low current IV curve tracer since they had leakage current in the tens of picoamperes. The Kyma devices were tested with fluorinert covering the top of the device up to 10 kV with a higher current IV curve tracer. As shown in Figures 3 and 4, the Ammono devices have approximately 4 - 5 orders of magnitude better off state resistance than the Kyma devices.

C. Surface Flashover Electric Field

The flashover of PCSS devices is an important parameter for testing devices, especially when the devices are tested in air, without a dielectric between the electrodes. The dielectric strength of the devices varies depending on the high voltage pulse width, but the Kyma Technologies and Ammono devices had a surface flashover electric field of approximately 30 kV/cm.

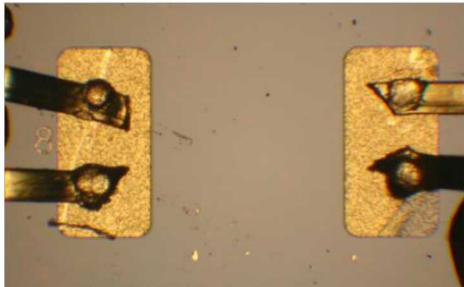


Fig. 2. Kyma PCSS singulated device die.

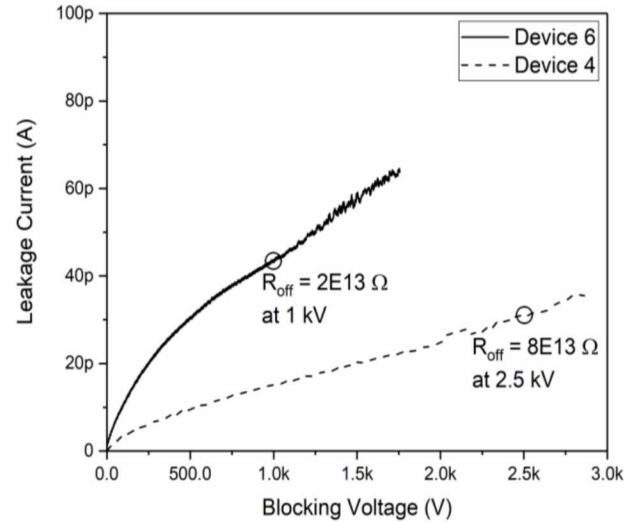


Fig. 3. Ammono PCSS dark leakage current.

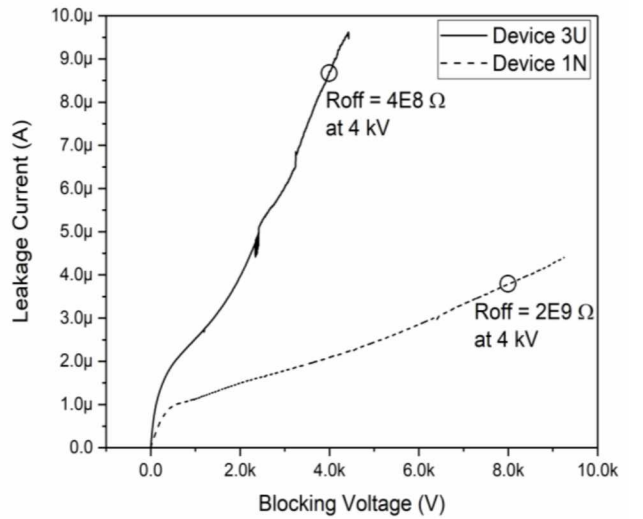


Fig. 4. Kyma PCSS dark leakage current.

III. PCSS TEST CONFIGURATION

The PCSS devices were tested in the circuit depicted in Figure 5. A dc power supply charged a DEI pulse generator to between 0 V – 2500 V. The DEI pulse generator was controlled with a DG535 to pulse charge a diode string and short RG-214 cable with approximately a 60 ns rise / fall time. A frequency doubled Nd:YAG Q-switched laser with a 6 ns pulse width was used as the optical trigger to the PCSS. The testing thus far on the PCSS devices have been switched at the sub-bandgap wavelength of 532 nm (bandgap wavelength is 365 nm). A 1 $\text{k}\Omega$ load resistance was used to keep the conduction current through the device below 2 A. A majority of the testing was performed with peak currents between 1 A and 1.5 A. Some testing was done in a single shot configuration, while a majority of the testing was performed at either 1 Hz or 20 Hz repetition rate testing.

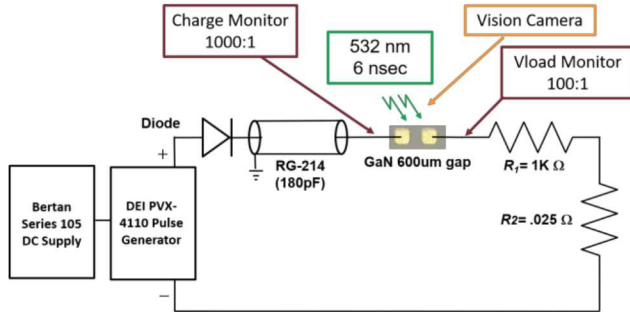


Fig. 5. PCSS test configuration.

The charge voltage, $1\text{ k}\Omega$ load voltage, and $0.025\text{ }\Omega$ CVR voltage were all recorded throughout testing. A color vision camera took images of the device during conduction to document filamentation and a photodetector recorded the timing of the laser pulse to the current conduction. Separate measurements of laser energy were measured prior to testing the devices.

IV. PCSS TEST RESULTS AND DISCUSSION

The GaN PCSS exhibits both linear and high-gain mode switching characteristics. High gain mode switching occurs when the device has an electric field above a specific value, called the lock-on field. The $600\text{ }\mu\text{m}$ gap PCSS devices outlined in this paper have a lock-on field of approximately 20 kV/cm . The waveforms presented in Figures 6 and 7 show the linear and high-gain mode switching characteristics, respectively.

The PCSS exhibits linear switching in Figure 6 because the current waveform follows the laser pulse with the current decay governed by carrier recombination. The charge voltage on the high side of the device has a slight droop, but not all of the energy from the transmission line was discharged through the device in the approximately 25 ns long current pulse. The peak current during linear mode operation is only 110 mA .

Figure 7 demonstrates high gain mode switching. Once lock-on is initiated from laser generated electron-hole pairs, avalanche carrier generation is sustained to maintain conduction even after the laser illumination is removed, until the electric field across the device decays below the minimum critical lock-on field of approximately 3 kV/cm (200 V). This is depicted in Figure 7. After the laser illumination is removed, the device remains conducting for an additional 410 ns and is on until the voltage on the high side of the device decays to 200 V . At this point, the conduction current drops to 0 A and the voltage across the device is maintained, indicating that the device has turned off.

This phenomenon has been demonstrated in GaN PCSS to be repeatable and laser induced in all our testing. However, this phenomenon has not yet been demonstrated with fluorinert covering the gap of the device. It has only occurred when the gap of the device is open to the air. This lends to the belief that in GaN, the high-gain mode switching is partially due to a surface effect that is no longer present when the device is submerged in fluorinert. Further investigation is

required to completely understand this mode of operation and is outside the scope of this manuscript.

A key aspect of high gain mode is the reduction in laser energy required to turn on the device. This is significant because it can greatly reduce the size of the laser and driver used for turning on the PCSS. Instead of an Nd:YAG Q-switched laser, a laser diode could be enough energy to drive the semiconductor. In testing, the linear mode switching was initiated with $100\text{ }\mu\text{J}$ of laser energy and delivered $3.5\text{ }\mu\text{J}$ of energy to the load, requiring more energy to turn on the device than was delivered. The high gain mode switching in Figure 7 was initiated with $33\text{ }\mu\text{J}$ of laser energy and delivered $256\text{ }\mu\text{J}$ of energy to the load, requiring much less energy to turn the device on than was delivered to the load. This allows for much more energy efficient switching with the additional benefit of smaller lasers. Note that the blue laser waveform in Figures 6 and 7 only show the timing of the laser pulse and does not correlate to the laser energy.

Filamentation is another typical characteristic of high-gain mode operation of PCSS. Linear mode operation allows for uniform conduction across the device, whereas high-gain mode causes filaments, or current channels, to form on the surface of and into the bulk of the device.

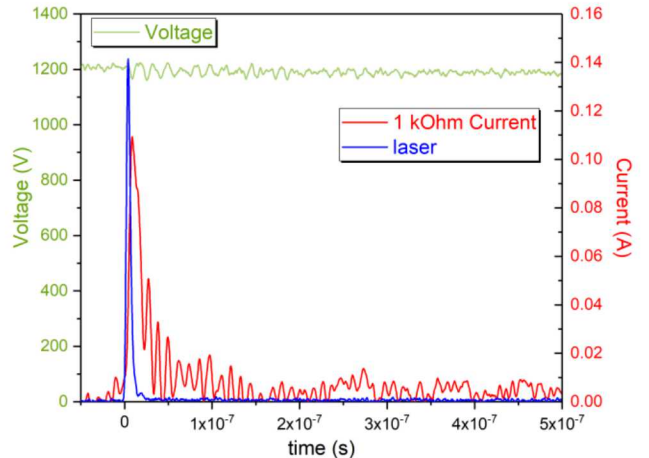


Fig. 6. Example linear mode switching waveform for a GaN PCSS.

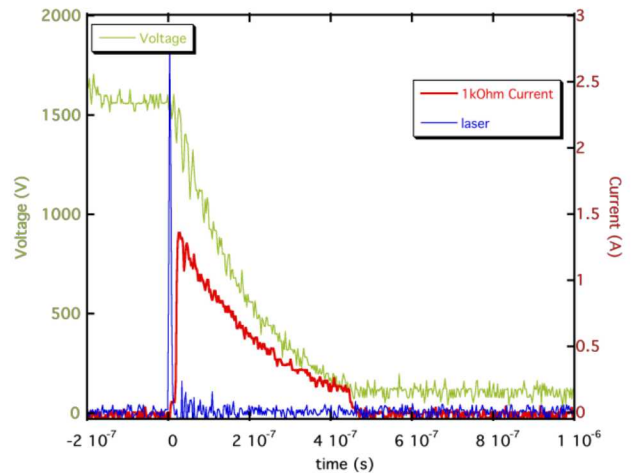


Fig. 7. Example high gain switching waveform for a GaN PCSS.

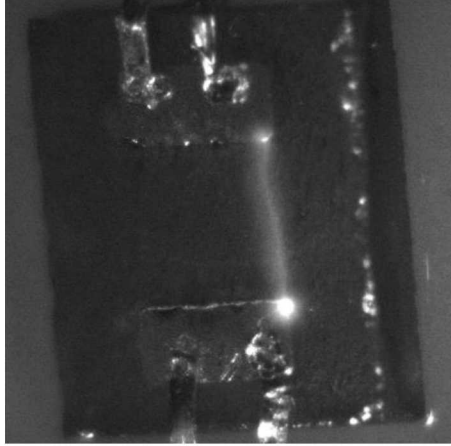


Fig. 8. Filamentary current conduction during a high gain mode switching event in GaN PCSS.

Filamentation has been observed in the GaN PCSS devices outlined in this paper during high-gain mode switching. Figure 8 shows the filamentation in the device during the Figure 7 cycle. As shown, there is a main filament that runs from each electrode of the device towards the right hand side. This filamentation can degrade the device significantly, as has been shown in GaAs PCSS devices [6], however, with GaN devices operating at low current conduction of approximately 1 A, the device has been tested to withstand hundreds of pulses.

V. CONCLUSION

GaN PCSS devices are a promising technology for repetitive power electronics or pulsed power applications. The material properties of GaN allow for higher voltage and more temperature robust devices. The ability for these devices to be switched in a high gain mode, where persistent conductivity occurs, allows for the use of smaller laser systems and more efficient device triggering. A GaN PCSS research grade device has been tested with over 900 low current (less than 1.5

A peak) 400 ns width pulses, which shows that it could be feasible to use in systems in the future. Some repetitive rate testing at 20 Hz has been accomplished to start testing the low current lifetime of these devices.

ACKNOWLEDGMENT

Sandia National Laboratories is a multimission laboratory managed and operated by National Technology & Engineering Solutions of Sandia, LLC, a wholly owned subsidiary of Honeywell International Inc., for the U.S. Department of Energy's National Nuclear Security Administration under contract DE-NA0003525. This paper describes objective technical results and analysis. Any subjective views or opinions that might be expressed in the paper do not necessarily represent the views of the U.S. Department of Energy or the United States Government.

REFERENCES

- [1] A. V. Bilbao *et al.*, "Continuous switching of ultra-high voltage silicon carbide MOSFETs," *2016 IEEE International Power Modulator and High Voltage Conference (IPMHVC)*, San Francisco, CA, 2016, pp. 463-466.
- [2] D. L. Mauch *et al.*, "Ultrafast Reverse Recovery Time Measurement for Wide-Bandgap Diodes," in *IEEE Transactions on Power Electronics*, vol. 32, no. 12, pp. 9333-9341, Dec. 2017.
- [3] E. A. Hirsch, J. A. Schrock, S. B. Bayne, H. O'Brien and A. Ogunniyi, "Narrow pulse evaluation of 15 KV SiC MOSFETs and IGBTs," *2017 IEEE 21st International Conference on Pulsed Power (PPC)*, Brighton, 2017, pp. 1-4.
- [4] J. A. Schrock *et al.*, "Failure Analysis of 1200-V/150-A SiC MOSFET Under Repetitive Pulsed Overcurrent Conditions," in *IEEE Transactions on Power Electronics*, vol. 31, no. 3, pp. 1816-1821, March 2016.
- [5] J. S. Sullivan and J. R. Stanley, "Wide Bandgap Extrinsic Photoconductive Switches," in *IEEE Transactions on Plasma Science*, vol. 36, no. 5, pp. 2528-2532, Oct. 2008.
- [6] W. Shi, C. Ma and M. Li, "Research on the Failure Mechanism of High-Power GaAs PCSS," in *IEEE Transactions on Power Electronics*, vol. 30, no. 5, pp. 2427-2434, May 2015.